Modelling, design, and control of a robotic running foot for footwear testing with flexible actuator

Do, Thanh Nho; Nguyen, Thanh Luan; Lau, Michael Wai Shing; Phee, Soo Jay

2014

Nguyen, T. L., Do, T. N., Lau, M. W. S., & Phee, S. J. (2014). Modelling, design, and control of a robotic running foot for footwear testing with flexible actuator. The 1st International Conference in Sports Science & Technology (ICSST), Singapore, 2014, 505-514.

https://hdl.handle.net/10356/103777

1st International Conference in Sports Science & Technology
ICSST
ADVANCED TECHNOLOGIES IN MODERN DAY SPORTS
11-12 Dec 2014 | Hotel Novotel Clarke Quay, Singapore

Sports Products Engineering for Sports Technology
www.icsst14.com

Modelling, design, and control of a robotic running foot for footwear testing with flexible actuator

T.L. Nguyen[1, 2], T.N. Do[2], M.W.S. Lau[3], S.J. Phee[2]

[1] *Institute for Sports Research, Nanyang Technological University, 50 Nanyang Avenue, Singapore,*

[2] *School of Mechanical and Aerospace Engineering, Nanyang Technological University, 50 Nanyang Avenue, Singapore*

[3] *School of Mechanical and Systems Engineering, Newcastle University, United Kingdom*

Abstract

Footwear effects on the human feet have been widely studied to prevent injuries, improve sports performance, and human health through running exercise. Due to the dynamics of human joints and passive imitative feet, current automatic footwear testing systems reported in the literature are not very realistic, are limited in the imitation of running gaits, and still use the passive prosthetic foot. In addition, many studies on humanoid walking robots, orthotic ankles, and prosthetic foot for amputees only focus on the human ankle joint and walking gaits. In this project, the design and control of a realistic robotic running foot-leg testing of shoes are introduced. The designed robotic foot possesses a higher number of degrees of freedom compared to other robotic systems in the literature and have abilities to mimic accurately biomechanical patterns of the human foot as well as to replicate the plantar pressure distribution under the foot sole in running in the sagittal plane. Because of lightweight, flexibility, and ease of power transmission, the Bowden-cable or the tendon-sheath mechanism (TSM) is used in this project for the actuation of the robotic joints. However, nonlinear friction and backlash hysteresis in such mechanisms vary with the change of cable configuration and they degrade the system performances. In this project, novel nonlinear and adaptive schemes for controlling the position of the ankle and metatarsophalangeal joints will also be presented. The control schemes consider the nonlinear and backlash hysteresis as uncertainties and are able to deal with unexpected disturbances due to the change of the cable configuration and the unknown environments. In addition, no knowledge of the model parameters is required. To validate the design systems and control approaches, simulations are also introduced. There are good agreements between the proposed approaches and simulation results.

1. Introduction

There are three main different approaches for footwear testing: human participant, virtual testing, and mechanical devices. Although human participant approach provides the most realistic condition for sports equipment testing; however, time consuming process,

performance variability, and small number of participated subjects and trials cause challenges in this testing method [1], [2]. Another alternative method for the footwear testing is the virtual testing approach (e.g. the finite element method). However, it has shown difficulties in the modelling approach under the presence of geometric complexity objects or uncertain boundary for the used materials [2], [4]. Because of its simple control and easy adjustment of the designed parameters as well as stable repeat in the testing process, mechanical devices can be considered as the most favourite method in the testing sports equipment. Nevertheless, they still lack of bio-fidelity for the human locomotion dynamics, especially in running gait.

Some studies on the footwear testing devices have been reported in the literature. Monckton *et al*. [5] used the Hexapod system to test the footwear shoe where actuators are simultaneously controlled to replicate the contact-phase interaction between the shoe and the ground. Ronkainen *et al.* [2] used a 6-DOF industrial robot (iRobot, Fanuc R-2000iB/165F) to replicate the foot-ground contact phase of the human with a prosthetic footwear testing shoe at the end effector. However, these robotic systems were not able to mimic the running gaits and even not able to reach the average running speed of the human (8 km/h to 12 km/h). Further, their end effectors were limited at a maximum speed of 2 m/s compared to actual wear trials of about 3.5 m/s [3].

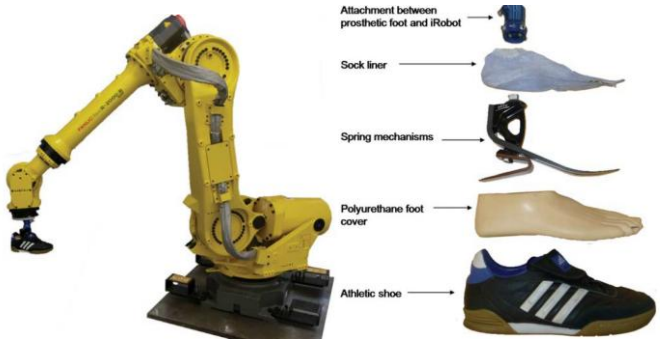

Figure 1. The automatic footwear testing system developed by Loughborough University **[2].** The left picture is the 6-DOF industrial robot from Fanuc while the right picture shows the structure of the prosthetic foot wearing the test shoe

The most applicable system for footwear testing is the STM 528 Pedatron™ developed by SATRA Technology Centre and it is recognised as the world's leading agency in footwear testing [6]. This system was able to control the horizontal position and angle of the shank as well as the foot height and impact force. In addition, it has proved capabilities of imitating the walking gait based on their abundant biomechanical database. However, STM 528 Pedatron™ was limited on imitating the walking gait and used the passive prosthetic feet (as shown in Figure 1) which lacks bio-fidelity to represent the interaction between the ground and the shoe during the gait cycle. Other innovative robotic feet developments including orthoses and prostheses can be found in [7], [8], [9], [10], [11], [12], [13], [14]. In a nutshell, the use of current actuators like series elastic actuators (SEA) in the above systems caused limitations on mimicking the human running gait and therefore degraded the system performances.

To overcome these above drawbacks, in this paper, a robotic footwear testing system for the human shoe and an efficient adaptive position control scheme will be developed and

discussed. The designed prototype for the prosthetic foot possesses similar size, weight, shape and appearance (i.e. the resilience of the foot sole) as the human foot and able to imitate the effect of human foot on the shoe realistically, especially the plantar pressure. In addition, it is able to replicate the movement of human foot and provide enough power for joint transmissions. To provide flexible transmission and low bulkiness for the designed system, Bowden-cable mechanism (BCM) or tendon-sheath mechanism (TSM) is used. This mechanism is preferred because it can operate in very limited space and narrow paths and allows for external provision of the actuator since the robotic joints are placed away from the actuation side. In addition, it is able to generate a high payload and easy implementations as well as offers simple design. Although the TSM offers advantages, the nonlinear friction and backlash hysteresis nonlinearities cause challenges in the precise control of position for the joints of the systems. Various modelling and compensation approaches in terms of position and tension transmissions for the TSM have been reported in the literature [15], [16], [17], [18], [19], [20], [21]. However, there still exist limitations on the model approach such as discontinuity for the tension transmission models, cable-conduit configuration must be known in advance. To relax these drawbacks, a novel position adaptive control scheme will be developed in this paper. The proposed control approach uses online estimation of model parameters and no knowledge of the parameters is required. To validate the nonlinear control scheme, relevant simulations will be also introduced.

2. Prototype Design for the Robotic Footwear Testing System

In this section, a novel prototype design for the foot-leg model with total five DOFs will be presented. The new design consists of Bowden-cable mechanisms-driven foot model with attached shank. A pair of BCMs is used to actuate a joint for both clockwise and counter clockwise directions. As can be seen from the Figure 2, the ankle drive pulley is used to control the motion/torque of the ankle pulley while the metatarsophalangeal joint (MTPJ) pulley is driven by the MTPJ drive pulley. Each of pair of the BCMs acts as a group of human foot-leg muscles to control the foot's joint. Specifically, the AT cable represents the role of the Achilles tendon and the group of gastrocnemius as well as soleus muscles while the TA cable is considered as the tibialis anterior muscle. Similarly, the TEX cable plays a role of the toe extensor muscle and the TFL which is simulated as the toe flexor muscle is used to control the angular position and torque of the MTPJ.

To provide position/torque to the joint pulleys, an AC brushless motor 115U2D300BACAA130240 which is connected to the ankle drive pulley via a coupling joint is used to actuate the ankle drive pulley. This motor in combination with a low-backlash gearbox GBPH-1202-NP-015 from Anaheim Automation is driven by a motor drive M701-03400100 from Control Technique. Similarly, an AC servo motor 075U2C300BACAA075140 connected to the gearbox GBPN-0802-032 from Anaheim Automation is integrated to the MTPJ drive pulley. To drive this AC servo motor 075U2C300BACAA075140, a motor drive M701-03400032 from Control Technique is also used. It is noted that the fixed parts of the drive pulleys are fixed on the ground while the joint pulleys are freely moved along a predefined trajectory (the human foot position during the running gait).

At the robotic foot, to minimise the effect of friction force between the cable and the conduit while maintaining the designed robotic foot in a similar size of the real foot, a timing belt transmission which is fixed to the foot is used. Using the AT cable and TA cable, the ankle drive pulley will control the big timing pulley via the ankle follower pulley. To measure the angular positions of the ankle joint and the MTPJ, a 12-bit absolute mini encoder SCH24AB-12G-06-50-03-IDC from SCANCON is mounted at each joint. The feedback signals from these encoders help to close the motion control loop of the ankle joint and MTPJ. The robotic foot is attached to the shank through a pyramid adapter at its top. Because the dynamic effect of the upper leg on the foot can be replicated by a three-degrees-of-freedom shank, a proposed shank mechanism is also developed as shown in Figure (a). This designed mechanism consists of three actuators which control two parallel translational motions (i.e. motion number 1 and 2) and an axial motion along the shank's axis. With the three motions generated by the shank mechanism, any translational position of the foot and the angular position between the shank and the ground can be flexibly evaluated. In order to estimate and compensate the friction force of the CCTs using the torque control technique, an incremental encoder SCH50F-4096-NON-08-26-65-01-S-00-S3 from SCANCON is used to measure the angular displacements at each drive pulley (i.e. the ankle drive pulley and MTPJ drive pulley). In addition, torque sensors FSH02059/TRS605 and FSH01990/TRS300 from Futek are also utilized. The former will measure the torque at the ankle drive pulley while the latter is used to monitor the torque at the MTPJ drive pulley. With the new prototype design, the robotic foot shows abilities to mimic accurately biomechanical patterns of the human foot as well as to replicate the plantar pressure distribution under the foot sole in running in the sagittal plane. However, the position control for the CCMs under the presence of nonlinear friction and backlash hysteresis is much more challenging. In the next section, a novel nonlinear adaptive control scheme will be developed to relax the current limitations in the use of the CCMs.

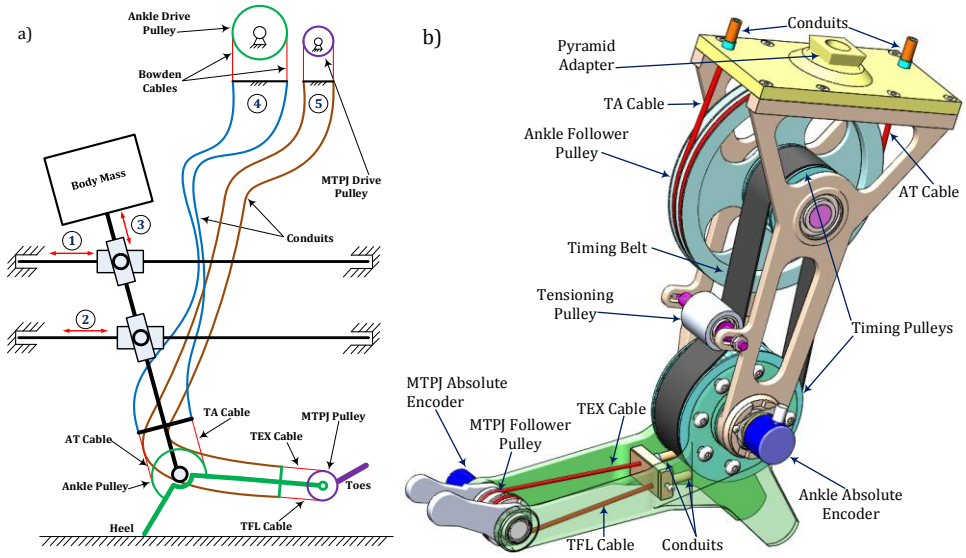

Figure 2. (a) Schematic of foot model actuated by cable-conduit transmissions in attachment with the shank mechanism. Three actuators (i.e. the translational movements 1 to 3) actuate the shank. The foot has two powered joints (No. 4 and 5) at the ankle joint and metatarsophalangeal joint (MTPJ). The Achilles Tendon (AT) cable and Tibialis Anterior (TA) cable control the ankle joint while the Toe Flexor (TFL) cable and Toe Extensor (TEX) cable actuate the MTPJ. (b) The CAD model of the robotic foot.

3. System Model Approach

The position transmission in the Bowden-cable mechanism can be modelled as introduced in Do *et al*. [19]:

$$y = cu + d + \Delta_n \tag{1}$$

where y denotes the displacement at the distal end of the TSMs; the displacement at the proximal end of the TSMs, u is the control input for the system, d represents the transition curves of backlash hysteresis profile, c is a positive coefficient which denotes the slope of backlash hysteresis profile, Δ_n denotes the uncertain disturbance caused by changes in the tendon-sheath configuration during experimental process.
The control objectives are to design a nonlinear position controller with adaptive update laws such that:

- The closed loop is globally stable in the sense that all the signals are uniformly bounded.
- The tracking error $e_r = y(t) - y_r(t)$ tends to compact regions by suitable choices of design parameters.

Let the positive value D^* be the bound of the function $D = d + \Delta_n$ which is assumed to be unknown. It will be estimated using the designed adaptive laws. Define a coordinate transformation n for the system given by Eq. (1) and a filter tracking error z as follows:

$$\begin{cases} n = \int_0^t \left(y(\tau) - y_r(\tau) \right) d\tau \\ e_r(t) = y(t) - y_r(t) \\ z = e_r(t) + \alpha \int_0^t e_r(\tau) d\tau \end{cases} \tag{2}$$

where α is an arbitrarily positive constant.
The first order derivative of the new variable z can be expressed by:

$$\dot{z} = \alpha \left(y - y_r \right) + \dot{e}_r = \alpha \left(cu + D - y_r \right) + \dot{e}_r \tag{3}$$

For the uncertainty given by Eq. (1), we proposed a new robust control scheme to counteract its effects. The adaptive control law with Nussbaum gain technique is designed as follows:

$$u = N(\zeta)\bar{u} \tag{4}$$

$$\bar{u} = mz + \frac{z}{|z| + \varepsilon e^{-\beta t}} \hat{D}^* - y_r + \frac{1}{\alpha} \dot{e}_r \tag{5}$$

$$\dot{\zeta} = \delta_1 \bar{u} z \tag{6}$$

$$\dot{\hat{D}}^* = \frac{\delta_2 z^2}{|z| + \varepsilon e^{-\beta t}} \tag{7}$$

where $m, \delta_1, \delta_2, \alpha$ are positive parameters that adjust the controller to force the tracking errors tend to zero value, $\varepsilon > 0, \beta > 0$ are the designed parameter for update law, $\tilde{D}^* = D^* - \hat{D}^*$ represents for the error estimate of bounded disturbance $D^*, N(\zeta)$ is the

Nussbaum function, $\bar{u}$ is a virtual control input. It is noted that the virtual controller $\bar{u}$ given by Eq. (6) utilized a smooth continuous function $\upsilon = z/(|z| + \varepsilon e^{-\beta t})$ as introduced in Qu [22]. In this section, all the signals in the system will be proven to be bounded. With the controller (4) to (5) and update laws (6) to (7), we define a Lyapunov function *V* as:

$$V = \frac{1}{2}z^2 + \frac{1}{2\mu}\tilde{D}^{*2} \tag{8}$$

Then the derivative of *V* is given by:

$$\dot{V} = z\dot{z} - \frac{1}{\mu}\tilde{D}^*\dot{\hat{D}}^* = z\left(\alpha\left(cN(\zeta)\bar{u} + D - y_r + \frac{1}{\alpha}\dot{e}_r\right) + \dot{e}_r\right) - \frac{1}{\mu}\tilde{D}^*\dot{\hat{D}}^*$$

$$= z\left(\alpha\left((cN(\zeta)+1)\bar{u} - \bar{u} + D - y_r + \frac{1}{\alpha}\dot{e}_r\right) + \dot{e}_r\right) - \frac{1}{\mu}\tilde{D}^*\dot{\hat{D}}^*$$

$$= z\left(\alpha\left((cN(\zeta)+1)\bar{u} - \left(mz + \frac{z}{|z| + \varepsilon e^{-\beta t}}\hat{D}^* - y_r + \frac{1}{\alpha}\dot{e}_r\right) + D - y_r\right) + \dot{e}_r\right) - \frac{1}{\mu}\tilde{D}^*\dot{\hat{D}}^*$$

$$= -m\alpha z^2 + \alpha(cN(\zeta)+1)\bar{u}z - \frac{\alpha z^2}{|z| + \varepsilon e^{-\beta t}}\hat{D}^* + D\alpha z - \frac{1}{\mu}\tilde{D}^*\dot{\hat{D}}^*$$

$$\le -m\alpha z^2 + (cN(\zeta)+1)\bar{u}z - \frac{\alpha z^2}{|z| + \varepsilon e^{-\beta t}}\hat{D}^* + D^*\alpha|z| - \frac{1}{\mu}\tilde{D}^*\dot{\hat{D}}^*$$

$$= -m\alpha z^2 + \alpha(cN(\zeta)+1)\bar{u}z - \frac{\alpha z^2}{|z| + \varepsilon e^{-\beta t}}\hat{D}^* + \frac{D^*\alpha z^2 + \varepsilon\alpha D^*|z|e^{-\beta t}}{|z| + \varepsilon e^{-\beta t}} - \frac{1}{\mu}\tilde{D}^*\dot{\hat{D}}^*$$

$$= -m\alpha z^2 + \alpha(cN(\zeta)+1)\bar{u}z + \left(\frac{\alpha z^2}{|z| + \varepsilon e^{-\beta t}} - \frac{1}{\mu}\dot{\hat{D}}^*\right)\tilde{D}^* + \frac{\varepsilon\alpha D^* e^{-\beta t}|z|}{|z| + \varepsilon e^{-\beta t}}$$

$$\le -m\alpha z^2 + \frac{1}{\delta}(cN(\zeta)+1)\alpha\delta\bar{u}z + \varepsilon\alpha D^* e^{-\beta t}$$

$$\Rightarrow \dot{V}(t) \le -m\alpha z^2 + \frac{1}{\delta}(cN(\zeta)+1)\dot{\zeta} + \varepsilon\alpha D^* e^{-\beta t} \tag{9}$$

Or $\dot{V}(t) \le -m\alpha z^2 + \frac{1}{\delta}(cN(\zeta)+1)\delta\alpha\bar{u}z + \varepsilon\alpha D^* e^{-\beta t} \le \frac{1}{\delta}(cN(\zeta)+1)\delta\alpha\bar{u}z + \varepsilon\alpha D^* e^{-\beta t}$ (10)

where $\dot{\hat{D}}^* = \frac{\delta_2 z^2}{|z| + \varepsilon e^{-\beta t}}$, $\delta_2 = \alpha\mu$, $\dot{\zeta} = \delta_1\bar{u}z$, $\delta_1 = \alpha\delta$.

Integrating (10) gives:

$$V(t) \le \int_0^t \frac{1}{\delta}(cN(\zeta(\tau))+1)\dot{\zeta}(\tau)d\tau + \int_0^t \varepsilon\alpha D^* e^{-\beta\tau}d\tau + \Lambda \tag{11}$$

According to Ye *et al.* [23], we have $\zeta(t)$ and $V(t)$ are bounded on $[0, t_f)$ due to the $\int_0^t \varepsilon\alpha D^* e^{-\beta\tau}d\tau = -\varepsilon\alpha D^* e^{-\beta t}/\beta\Big|_0^t = \varepsilon\alpha D^*/\beta$ as $t \to \infty$. These results guarantee the boundedness of $z, \tilde{D}^*, D^*$, and $\hat{D}^*$. In the same argument, the boundedness of control input *u* is guaranteed. One again, integrating Eq. (9) gives:

$$V(t) \le -m\alpha \int_0^t z^2(\tau)d\tau + \int_0^t \frac{1}{\delta}\left(cN(\zeta(\tau))+1\right)\dot{\zeta}(\tau)d\tau + \int_0^t \varepsilon\alpha D^* e^{-\beta\tau}d\tau + \theta \qquad (12)$$

where θ is some constants.

We can see that the variable z is square-integrable and bounded. Hence, its components such as $n, \dot{n}$ are also integrable. From Babalat's lemma we can conclude that $\lim_{t\to\infty}|z| = 0$, $\lim_{t\to\infty} n = 0$, and $\lim_{t\to\infty} \dot{n} = \lim_{t\to\infty} e_r = 0$. Hence, asymptotic tracking is achieved.

4. Simulation Results

In this section, we present the simulation results for proposed control schemes. The results promise efficient improvements for tracking performances of nonlinearities for the CCMs. The uncertainties and disturbances D for the symmetric backlash hysteresis can be chosen by:

$$\dot{D} = -0.9162\dot{y}_r - 10.1062|\dot{y}_r|D \qquad (13)$$

where y_r represents for the desired trajectory.

For simulation purpose, the slope is chosen as $c = 1.012$. The objective is to control the output displacement y to follow the desired trajectory $y_r = 0.4\sin(0.6\pi t) + 0.4\sin(0.25\pi\sqrt{3}t)$ as close as possible. The updated parameters are chosen with $m = 30$, $\varepsilon = 1$, $\beta = 0.01$, $\delta_1 = 100$, $\delta_2 = 10$, $\alpha = 5$. The initial values for estimated variables are chosen to $\zeta(0) = 1$ and $\hat{D}^*(0) = 0$. The Nussbaum function in this case is $N(\zeta) = \zeta^2\cos(\zeta)$. Figure 3 shows the simulation results for the first control scheme. The left panel of this figure presents the time history of the desired trajectory y_r and output displacement y. It can be observed that the output follows the desired trajectory accurately after a few periods. The corresponding error is also introduced in this figure. The right panel of Figure 3 illustrates the time history of the control input and estimate update variables. It can be also proven that the proposed control schemes for the backlash hysteresis in the TSM has been successfully validated with a good agreement for the tracking error between the output and desired trajectory.

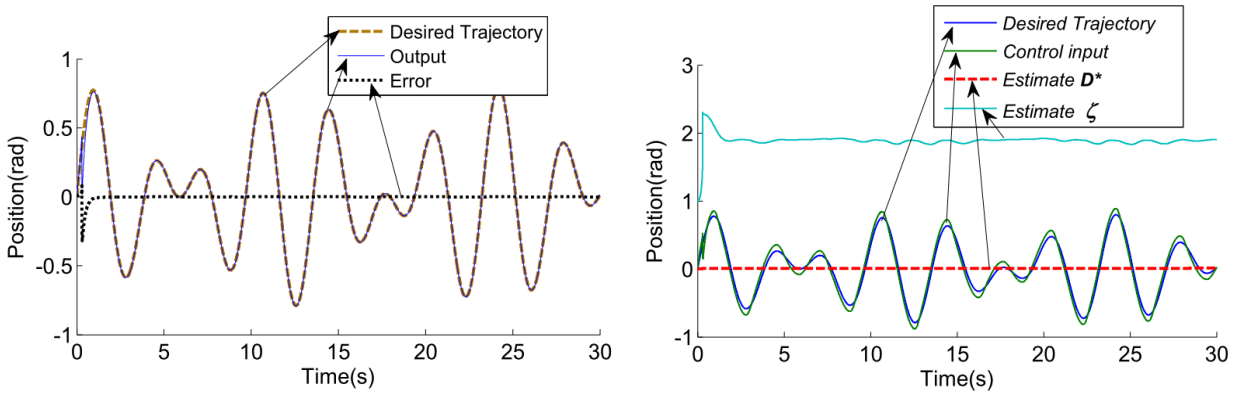

Figure 3. Numerical simulation result for the proposed control nonlinear adaptive scheme.

5. Discussions and Conclusion

Many studies reported in the literature on the humanoid walking robots, orthotic ankles, and prosthetic foot for amputees only focus on the human ankle joint and walking gaits. Due to the dynamics of human joints and the passive imitative feet, current automatic footwear testing systems are still limited in the imitation of running gaits and not very realistic as well as still use the passive prosthetic foot. The use of conventional motor at the robotic joints also causes the system bulkiness, high cost, and less flexibility in the testing system. Motivated from the current limitations in the footwear testing system, the design and control of a realistic robotic running foot-leg testing of shoes using the flexible cable-conduit mechanisms have been introduced. The designed system possesses a higher number of degrees of freedom of novel robotic foot compared to other robotic systems in the literature and has proven abilities to mimic accurately biomechanical patterns of the human foot as well as to replicate the plantar pressure distribution under the foot sole in running in the sagittal plane. To enhance the position tracking performances using the CCMs as the main mode of transmission, an efficient nonlinear and adaptive control scheme has been designed and discussed. The proposed control scheme is able to eliminate the nonlinear backlash hysteresis nonlinearities regardless of the use of cable-conduit configuration. In addition, no knowledge of model parameters is required for the designed control schemes. Only their bounds are online estimated. The proposed control scheme is successfully validated on simulation.

Although the designed prototype and control scheme have shown potential capabilities on the footwear testing system, only simulation and CAD model have been presented. For the future work, real-time experiments for the designed system and control scheme will be implemented. In addition, torque control for the CCMs will be also developed. Clinical trials on the human will be also carried out.

References

[1] Odenwald, S., Test Methods in the Development of Sports Equipment, in The Engineering of Sport 6. 2006, Springer New York. p. 301-306.
[2] Ronkainen, J.A., et al., Application of an industrial robot in the sports domain: Simulating the ground contact phase of running. Proceedings of the Institution of Mechanical Engineers, Part P: Journal of Sports Engineering and Technology, 2010. 224(4): p. 259-269.
[3] Heidenfelder, J., T. Sterzing, and T.L. Milani, Biomechanical wear testing of running shoes. Footwear Science, 2009. **1**(sup1): p. 16-17.
[4] Cheung, J.T.-M., et al., Current methods in computer-aided engineering for footwear design. Footwear Science, 2009. **1**(1): p. 31-46.
[5] Monckton, S.P. and K. Chrystall, Design and development of an automated footwear testing system, in Proceedings of the 2002 IEEE International Conference on Robotics and Automation. 2002. p. 3684-3689.
[6] SATRA-Technology. SATRA STM 528 Pedatron. [cited 2013 August 5]; Available from: http://www.satra.co.uk/portal/test_equipment/pedatron.php.
[7] Herr, H.M. and A.M. Grabowski, Bionic ankle-foot prosthesis normalizes walking gait for persons with leg amputation. Proceedings of the Royal Society B: Biological Sciences, 2012. **279**(1728): p. 457-464.
[8] Bellman, R.D., M.A. Holgate, and T.G. Sugar. SPARKy 3: Design of an active robotic ankle prosthesis with two actuated degrees of freedom using regenerative

kinetics. in 2nd Biennial IEEE/RAS-EMBS International Conference on Biomedical Robotics and Biomechatronics. 2008.

[9] Sup, F., H.A. Varol, and M. Goldfarb, Upslope Walking With a Powered Knee and Ankle Prosthesis: Initial Results With an Amputee Subject. EEE Transactions on Neural Systems and Rehabilitation Engineering, 2011. 19(1): p. 71-78.

[10] Lawson, B., et al., Control of Stair Ascent and Descent With a Powered Transfemoral Prosthesis. Neural Systems and Rehabilitation Engineering, IEEE Transactions on, 2013. 21(3): p. 466-473.

[11] Huff, A.M., B.E. Lawson, and M. Goldfarb. A running controller for a powered transfemoral prosthesis. in 34th Annual International Conference of the IEEE Engineering in Medicine and Biology Society. 2012. San Diego, CA.

[12] Cherelle, P., et al. The AMP-Foot 2.0: Mimicking intact ankle behavior with a powered transtibial prosthesis. in The Fourth IEEE RAS/EMBS International Conference on Biomedical Robotics and Biomechatronics. 2012. Rome, Italy.

[13] Collins, S.H. and A.D. Kuo, Recycling energy to restore impaired ankle function during human walking. PLoS ONE, 2010. 5(2).

[14] Grimmer, M., et al. A comparison of parallel- and series elastic elements in an actuator for mimicking human ankle joint in walking and running. in 2012 IEEE International Conference on Robotics and Automation. 2012. Minnesota, USA.

[15] V. Hassani, T. Tjahjowidodo, and T. N. Do, A survey on hysteresis modeling, identification and control, Mechanical Systems and Signal Processing, vol. 49, no. 1, pp. 209–233, 2014.

[16] V. Agrawal, W. J. Peine, and B. Yao, Modeling of transmission characteristics across a cable-conduit system, IEEE Transactions on Robotics, vol. 26, no. 5, pp. 914–924, 2010.

[17] T. N. Do, T. Tjahjowidodo, M. W. S. Lau, and S. J. Phee, An investigation of friction-based tendon sheath model appropriate for control purposes, Mechanical Systems and Signal Processing, vol. 42, no. 1-2, pp. 97–114, 2014.

[18] T. N. Do, T. Tjahjowidodo, M. W. S. Lau, and S. J. Phee, Nonlinear modeling and parameter identification of dynamic friction model in tendon sheath for flexible endoscopic systems, Proceedings of the 10th International Conference on Informatics in Control, Automation and Robotics (ICINCO), Reykjavik, Iceland, 2013, pp. 5–10.

[19] T. N. Do, T. Tjahjowidodo, M. W. S. Lau, T. Yamamoto, and S. J. Phee, Hysteresis modeling and position control of tendon-sheath mechanism in flexible endoscopic systems, Mechatronics, vol. 24, no. 1, pp. 12 –22, 2014.

[20] G. Palli, G. Borghesan, and C. Melchiorri, Modeling, identification, and control of tendon-based actuation systems, IEEE Transactions on Robotics, vol. 28, no. 2, pp. 277–290, 2012.

[21] T. N. Do, T. Tjahjowidodo, M. W. S. Lau, and S. J. Phee, Adaptive Control of Position Compensation for Cable-Conduit Mechanism Used in Flexible Surgical Robots, Proceedings of the 11th International Conference on Informatics in Control, Automation and Robotics (ICINCO). Vienna, Austria, 2014, pp. 110-117.

[22] Z. Qu, Robust Control of Nonlinear Uncertain Systems, John Wiley & Sons, Inc., New York, NY, USA., 1998.

[23] T. N. Do, T. Tjahjowidodo, M. W. S. Lau, S. J. Phee, A Novel Approach of Friction Model for Tendon-Sheath Actuated Surgical Systems: Nonlinear Modeling and Parameter Identification, Mechanism and Machine Theory, Vol. 85, pp. 14-24, 2015

[24] T. N. Do, T. Tjahjowidodo, M. W. S. Lau, S. J. Phee, Dynamic Friction Model for Tendon-Sheath Actuated Surgical Robot: Modeling and Stability Analysis, Proc. of the 3rd IFToMM International Symposium on Robotics and Mechatronics (ISRM 2013), Singapore, 2013, pp. 302-311

[25] X. Ye, J. Jiang, Adaptive nonlinear design without a priori knowledge of control directions, IEEE Transactions on Automatic Control, 43 (1998) 1617-1621